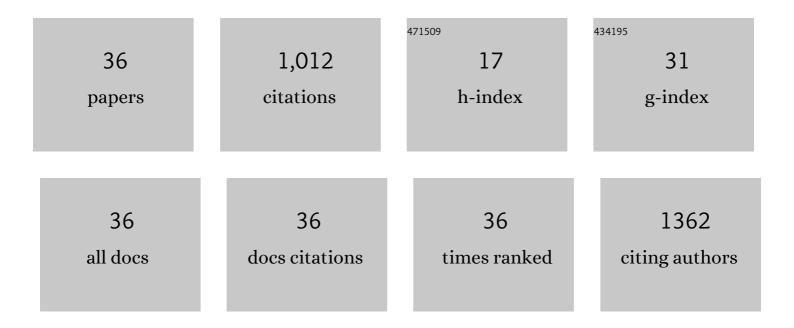
## Qingbiao Zhao

List of Publications by Year in descending order

Source: https://exaly.com/author-pdf/2749026/publications.pdf Version: 2024-02-01



#	Article	IF	CITATIONS
1	A Robust Artificial Synapse Based on Organic Ferroelectric Polymer. Advanced Electronic Materials, 2019, 5, 1800600.	5.1	129
2	A dual-template imprinted polymer electrochemical sensor based on AuNPs and nitrogen-doped graphene oxide quantum dots coated on NiS2/biomass carbon for simultaneous determination of dopamine and chlorpromazine. Chemical Engineering Journal, 2020, 389, 124417.	12.7	107
3	MOF-Derived NiO/NiCo <sub>2</sub> O <sub>4</sub> and NiO/NiCo <sub>2</sub> O <sub>4</sub> -rGO as Highly Efficient and Stable Electrocatalysts for Oxygen Evolution Reaction. ACS Sustainable Chemistry and Engineering, 2018, 6, 12511-12521.	6.7	79
4	Graphene oxide-Fe3O4 nanocomposite magnetic solid phase extraction followed by UHPLC-MS/MS for highly sensitive determination of eight psychoactive drugs in urine samples. Talanta, 2020, 206, 120212.	5.5	57
5	Rational Construction of a Ni/CoMoO <sub>4</sub> Heterostructure with Strong Ni–O–Co Bonds for Improving Multifunctional Nanozyme Activity. ACS Nano, 2022, 16, 4536-4550.	14.6	55
6	Smartphone based platform for ratiometric fluorometric and colorimetric determination H2O2 and glucose. Sensors and Actuators B: Chemical, 2020, 305, 127524.	7.8	53
7	C <sub>3</sub> N <sub>4</sub> Nanosheets/Metal–Organic Framework Wrapped with Molecularly Imprinted Polymer Sensor: Fabrication, Characterization, and Electrochemical Detection of Furosemide. ACS Sustainable Chemistry and Engineering, 2018, 6, 16847-16858.	6.7	49
8	Ratiometric fluorescence based on silver clusters and N, Fe doped carbon dots for determination of H2O2 and UA: N, Fe doped carbon dots as mimetic peroxidase. Sensors and Actuators B: Chemical, 2019, 287, 408-415.	7.8	46
9	Sensitive and rapid determination of glyphosate, glufosinate, bialaphos and metabolites by UPLC–MS/MS using a modified Quick Polar Pesticides Extraction method. Forensic Science International, 2018, 283, 111-117.	2.2	44
10	Colorimetric and fluorometric determination of uric acid based on the use of nitrogen-doped carbon quantum dots and silver triangular nanoprisms. Mikrochimica Acta, 2018, 185, 281.	5.0	39
11	Colorimetric determination of glutathione in human serum and cell lines by exploiting the peroxidase-like activity of CuS-polydopamine-Au composite. Analytical and Bioanalytical Chemistry, 2018, 410, 4805-4813.	3.7	34
12	Colorimetric and fluorometric dual-signal determination of dopamine by the use of Cu-Mn-O microcrystals and C-dots. Sensors and Actuators B: Chemical, 2019, 290, 125-132.	7.8	33
13	Flowerâ€like Ni(II)â€based Metalâ€organic Frameworkâ€decorated Ag Nanoparticles: Fabrication, Characterization and Electrochemical Detection of Glucose. Electroanalysis, 2019, 31, 2179-2186.	2.9	24
14	Molecularly imprinted polydopamine modified with nickel nanoparticles wrapped with carbon: fabrication, characterization and electrochemical detection of uric acid. Mikrochimica Acta, 2019, 186, 414.	5.0	22
15	A bifunctional NiCo <sub>2</sub> S <sub>4</sub> /reduced graphene oxide@polyaniline nanocomposite as a highly-efficient electrode for glucose and rutin detection. New Journal of Chemistry, 2018, 42, 9398-9409.	2.8	21
16	Colorimetric detection of gallic acid based on the enhanced oxidaseâ€like activity of floralâ€like magnetic Fe <sub>3</sub> O <sub>4</sub> @MnO <sub>2</sub> . Luminescence, 2019, 34, 55-63.	2.9	21
17	Single-Composition White Light Emission from Dy3+ Doped Sr2CaWO6. Materials, 2019, 12, 431.	2.9	20
18	Sensitive and rapid determination of pyrethroids in human blood by gas chromatography–tandem mass spectrometry with ultrasoundâ€assisted dispersive liquidâ€liquid microextraction. Drug Testing and Analysis, 2018, 10, 1131-1138.	2.6	17

**QINGBIAO** ZHAO

#	Article	IF	CITATIONS
19	Blue emission from Sr0.98Ga2B2O7: 0.01Bi3+, 0.01Dy3+ phosphor with high quantum yield. Journal of Alloys and Compounds, 2019, 810, 151849.	5.5	17
20	A fluorometric and colorimetric method for determination of trypsin by exploiting the gold nanocluster-induced aggregation of hemoglobin-coated gold nanoparticles. Mikrochimica Acta, 2019, 186, 272.	5.0	17
21	Sensitive determination of nine anticoagulant rodenticides in blood by high resolution mass spectrometry with supported liquid extraction pretreatment. Forensic Science International, 2018, 292, 39-44.	2.2	15
22	A ratiometric fluorometric and colorimetric probe for the $\hat{l}^2$ -thalassemia drug deferiprone based on the use of gold nanoclusters and carbon dots. Mikrochimica Acta, 2018, 185, 442.	5.0	15
23	Simultaneous determination of 16 alkaloids in blood by ultrahigh-performance liquid chromatography-tandem mass spectrometry coupled with supported liquid extraction. Journal of Chromatography B: Analytical Technologies in the Biomedical and Life Sciences, 2019, 1128, 121789.	2.3	13
24	Role of Loneâ€Pairs in Driving Ferroelectricity of Perovskite Oxides: An Orbital Selective External Potential Study. Advanced Theory and Simulations, 2019, 2, 1900029.	2.8	11
25	A dualâ€readout nanosensor based on biomassâ€based Câ€dots and chitosan@AuNPs with hyaluronic acid for determination of hyaluronidase. Luminescence, 2020, 35, 43-51.	2.9	11
26	Rapid and sensitive determination of formamidines and metabolites with HPLC-MS/MS using core-shell columns. Journal of Chromatography B: Analytical Technologies in the Biomedical and Life Sciences, 2018, 1076, 22-28.	2.3	10
27	Simultaneous determination of nine anticoagulant rodenticides by ultra-performance liquid chromatography–tandem mass spectrometry with ultrasound-assisted low–density solvent dispersive liquid–liquid microextraction. Journal of Chromatography B: Analytical Technologies in the Biomedical and Life Sciences. 2018, 1092, 453-458.	2.3	10
28	Sensitive, rapid and non-derivatized determination of glyphosate, glufosinate, bialaphos and metabolites in surface water by LC–MS/MS. SN Applied Sciences, 2019, 1, 1.	2.9	10
29	Sensitive and simultaneous determination of nine anticoagulant rodenticides in human blood by UPLC–MS-MS with phospholipid removal pretreatment. Journal of Analytical Toxicology, 2018, 42, 459-466.	2.8	8
30	Graphene transparent conductive films directly grown on quartz substrates by assisted catalysis of Cu nanoparticles. Journal of Materials Science, 2019, 54, 10312-10324.	3.7	8
31	Simultaneous determination of amitraz, chlordimeform, formetanate and metabolites in human blood by liquid chromatography tandem mass spectrometry with phospholipidâ€removal pretreatment. Biomedical Chromatography, 2019, 33, e4477.	1.7	6
32	Preparation and multiferroicity of a novel two-dimensional material NiH <sub>2</sub> SeO <sub>4</sub> . Journal of Materials Chemistry C, 2020, 8, 14812-14818.	5.5	5
33	Ferroelectric Synapses: A Robust Artificial Synapse Based on Organic Ferroelectric Polymer (Adv.) Tj ETQq1 1 0.7	'84314 rgE	3T / <sub>3</sub> Overlock
34	Non- <mml:math xmlns:mml="http://www.w3.org/1998/Math/MathML"&gt; <mml:msup> <mml:mi>d</mml:mi> <mml:mn>0ferroelectricity from semicovalent superexchange in bismuth ferrite. Physical Review B, 2021, 104, .</mml:mn></mml:msup></mml:math 	n> <b>⊲/ıı₂ml:</b> m	ารน <sub>ั</sub> p>
35	The Evolution of Amitraz and Its Metabolic Degradation Products in Human Blood over 90 Days for Use in Forensic Determination. Journal of Analytical Toxicology, 2020, 45, 937-942.	2.8	0
36	Nonreciprocal directional dichroism in multiferroics. Science China: Physics, Mechanics and Astronomy, 2020, 63, 1.	5.1	0